Acta of Bioengineering and Biomechanics
Vol. 13, No. 2, 2011

Original paper

Bone segmentation applying rigid bone position and triple shadow check method based on RF data

A. DOCTOR[1], BERNHARD VONDENBUSCH[1], JOSEF KOZAK[2]*

[1] Hochschule Furtwangen University, Department of Mechanical and Process Engineering, Germany.
[2] Aesculap AG, Tuttlingen, Germany.

Noninvasive 3D reconstruction of a bone requires very accurate 2D navigated scans of bone. The use of brightness-mode ultrasound seems to be promising, if some 2D scans of bone are obtained in a fully automatic manner. This paper presents a rapid and fully automatic method for segmenting bone in a standard 2D ultrasound image (B-mode image). The algorithm focuses on segmenting bone in the B-mode image using RF data of the image. The article introduces the signal-processing scheme designed based on RF data to automatically segment bone in the B-mode image. The segmentation accuracy was assessed by performing various tests for this algorithm for various locations of the limbs of the human body. The algorithm was tested for 120 images taken at different locations of limbs of the human body. The sensitivity of these tests was calculated to be 0.99 and specificity was found to be 1. The suggested segmentation approach provides a reliable means of detecting bone in B-mode image.

Key words: *ultrasound, automatic bone segmentation, RF data*

1. Introduction

3D bone visualization using CT is a well established method in the orthopaedics. But CT has some challenges when performed intraoperatively. In such a case, ultrasound offers a better solution for 3D bone visualization. A series of 2D segments from a sequence of B-mode images of a bone can be combined to form a 3D reconstructed bone, provided that the 2D scans of the bone are navigated. So the first task is to segment this bone in B-mode image of ultrasound. The target of this work described here is to visualize 2D segments of the bone in a B-mode image of ultrasound.

One of the most critical problems with ultrasound is to visualize bone. In the case of CT, the gray values are calibrated in accordance with the tissue, but such a calibration does not exist in the case of ultrasound. So we do not have a specific gray level for bones in a 2D ultrasound image. Therefore, segmenting a bone contour from all other structures in a B-mode image poses a real challenge.

Several groups have proposed the methods for automatic ultrasound bone segmentation. AMIN et al. [1] advocated the use of an initial registration in conjunction with the CT dataset to deliver an initial estimation of the image area that contains the bony surface. An edge detector was then utilized to extract the actual bone contour.

THOMAS et al. [2] proposed an automatic segmentation approach, mainly based on morphological operations, to estimate the femur length in fetal ultrasound images. The results reported indicate the conformity between the automatically calculated length of the femur and that manually determined. The time required for processing one single image which was 10 min would not be acceptable, but of course with the advancement in computer hardware the shorter timings than the published ones are very likely.

* Corresponding author: Josef Kozak, Aesculap AG, Am Aesculap Platz, 78532 Tuttlingen, Germany. Phone: +49 (7461) 95-2708, e-mail: Josef.Kozak@aesculap.de

Received: March 5th, 2011
Accepted for publication: April 29th, 2011

The use of fuzzy logic in combination with a priori knowledge about the osseous interface and ultrasound imaging physics to segment automatically ultrasound image was suggested by DAANEN et al. [3]. By using spatially separated ultrasound images, JAIN et al. [4] investigated the exact location of the osseous interface in relation to the echo produced. They further proposed an automatic bone surface detection method, using a Bayesian probabilistic framework.

In this article, a fully automatic bone segmentation algorithm for ultrasound image is described. The algorithm works on RF data to segment the bone structure. The algorithm proposed should be applicable to bones at any location in the body. So no a priori information about the bone to be segmented has been included. In the end, the algorithm is tested for a number of cases at different location of the limbs of the human body. The segmented bone is highlighted in the B-mode image.

2. Materials and methods

2.1. Procedure

The procedure adopted by us to segment the bone is described by the following steps.

1. We take the ultrasound pictures with the device called "SonixRp". The probe used has the length of 40 mm and the centre frequency of 10 MHz. We take the probe to any arbitrary position on the limbs and take the ultrasound image by adjusting the power in such a way as to obtain the minimum of speckle in the image. We call this image a image without pressure.

2. Without shifting the probe, we apply pressure randomly to the probe such that we feel that the probe is pressing the body. We store this picture too and we call it a image with pressure.

3. Now we provide our algorithm written in MATLAB with these two images taken above.

4. The algorithm gives the image with pressure as the output along with the highlighted bone surface.

The algorithm developed for bone segmentation works in two parts. The first part of the algorithm judges whether the two images (with and without pressure) have bone surface in them or not. If the images have no bone surface in them, then they abort the algorithm by giving a message to the user about the images having no bone surface in them.

The second part of the algorithm segments the bone surface from the two images.

We name the first part of the algorithm the *triple shadow check*, because this part of the algorithm checks whether the images contain bone structure or not by tracking the structures in the image from three different directions.

The second part of the algorithm is termed *rigid bone position*, wherein we isolate the bone from other structures in the image as the bone does not change its position in the body between the image with pressure and without pressure.

The two methods mentioned above are discussed in detail as follows.

2.2. Triple shadow check

This method is based on the basic idea of Spatial Compound imaging technique in ultrasound. Spatial compound imaging is an ultrasound technique that uses electronic beam steering a transducer array to rapidly acquire several overlapping scans of an object from different angles of view. These single-angle scans are averaged to form a multiangle compound image that is updated in real time with each subsequent scan. Compound imaging shows improved image quality compared with conventional ultrasound, primarily because of the reduction of speckle, clutter, and other acoustic artefacts.

In the case of *triple shadow check*, we do not take two or three images at different angles. In our algorithm, we just have two images: one is with pressure and one is without it.

So we begin with the image with pressure. In our algorithm, we work with RF data. So we take the first RF line from the left of our image with pressure and we start to track echo from the end of the line. In other words we can say that we start to look for the echo from the bottom and moving towards the top. As soon as an echo occurs we stop our search and store this echo in a new array. Then we move towards the next RF line, repeat the procedure and store the identified echo in the same new array. The procedure is continued until we reach the last RF line of the image. The image obtained after this procedure is shown in figure 1c. The arrows show the direction of scan.

In a way similar to the above procedure of echo tracing, we deal with a straight line. We look for the echo from right bottom end of the image and towards left-top corner. So we are scanning the image for the first echo found in a minus 45-degree direction. The image after this procedure is shown in figure 1b. In a similar fashion we scan the image for the first echoes in a positive 45-degree direction. The image after

this procedure is shown in figure 1a. The arrows in figure 1a and b show the direction of the scan. In the case of *triple shadow check* method, we tried to record the ultrasound image at various angles, i.e., 30° and 60°, but the best results were obtained for 45° scans. So we use 45° for scanning the structures in the image.

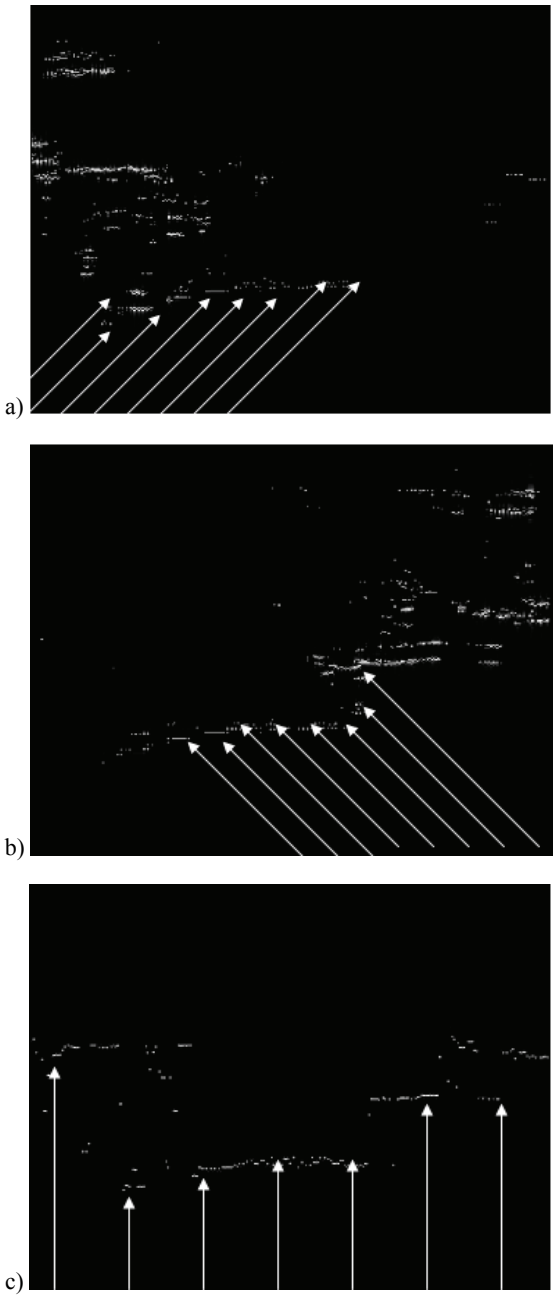

Fig. 1. Image showing 45° search for echo from left-bottom corner (a). Image showing minus 45° search for echo from right-bottom corner (b). Image showing bottom-up search for echo (c). All the three figures show significant bone structures. The structures above the bone are shadowed by the bone as the algorithm stops the search for echoes once it encounters a significant echo. So we see no significant structure above the bone

In *triple shadow check* method, we observe the shadow cast by significant structures when the image is scanned in three different directions from the bottom. In figure 1a, the scanning is from the left bottom and so one can observe the shadow in the right-upper portion of the image. Similarly, in figure 1b, as the scanning is from the right-bottom, one can easily observe the shadow in the upper-left corner of the image. In figure 1c, as the scan for the structures is from bottom towards the top, one can observe the shadow in the upper portion of the image.

Now we apply AND operation to these three images (a), (b) and (c). One important thing to be noted is that only the bone surface is the constant structure in all these three images in figure 1. So when we apply AND operation to these images only the common structure prevails, and the rest of the other uncommon structures are deleted. Thus, finally, after the AND operation we have the image shown in figure 2 with only the bone surface remaining after the AND operation.

After performing this procedure on our image with pressure we now proceed to the image without pressure and perform exactly the same steps as those mentioned above. So, finally, we obtain one more image after the AND operation which is similar to that in figure 2.

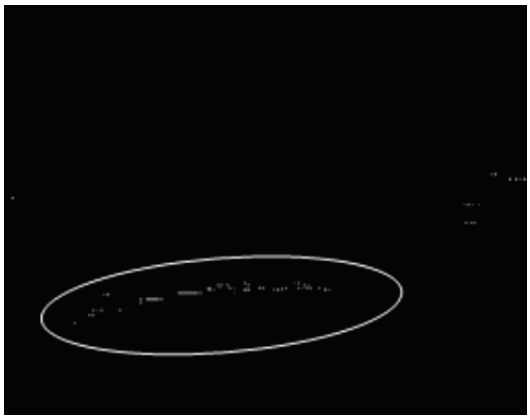

Fig. 2. Final image after AND operation on images obtained from different trace angles. The figure clearly shows bone structure as this bone structure is common to all the three images of *triple check* method while all the other significant structures no longer exist in the above image

Now we apply OR operation to these final two images. The resulting image is shown in figure 3. As can be seen, we just have two bone surfaces one beneath the other. So our algorithm judges that there are two similar structures one beneath the other. So this can happen, provided that the two structures are bone sur-

faces. Hence, the algorithm concludes that there is bone in the images and moves on to the next part, i.e., *rigid bone position*.

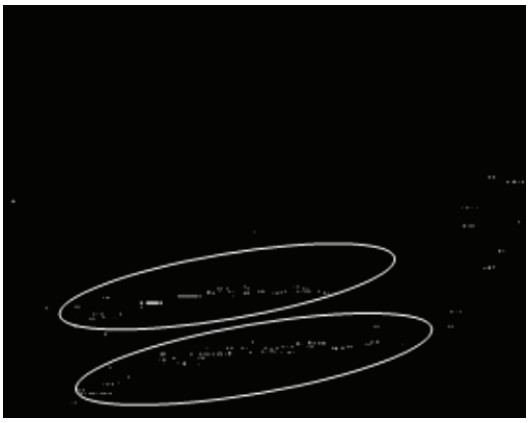

Fig. 3. Image obtained by logical summarizing (OR) the two images obtained from *triple check* method. The figure clearly shows two bone structures one beneath the other. The one at the top is from image with pressure and the bottom one is from the image without pressure

2.3. Rigid bone position

As soon as the bone echo in the image is confirmed, the algorithm moves on to the second part which is the *rigid bone position*. The basis of this part of the algorithm is elastography. In elastography, we take two images, one with pressure and one without it, in order to differentiate cancerous tissues (which are hard) from the normal body tissues (which are soft) (OPHIR et al. [10]). In elastography, we focus on the fact that the cancerous tissue is hard, so it demonstrates the minimum of strain in comparison to normal body tissues. However, in this method we base our algorithm on the fact that the bone is a rigid structure whose position and shape cannot be changed under the influence of arbitrarily slight pressure.

Let us observe the two ultrasound images in figure 4. Image (a) is without pressure, and image (b) is with pressure. The oval represents the bone surface. One very important observation is that the bone surface moves upwards in the image with pressure as compared to bone surface in the image without pressure. This happens because when we apply pressure the ultrasound probe moves downwards and the soft structures like skin and muscle move also downwards or get deformed. But the bone is the only rigid structure and a slight pressure cannot change its position or shape. Hence, in the image, it uniformly moves upwards. This is the peculiarity of the bone which makes it distinguishable from the rest of the structures. This behaviour of the bone in the images with and without pressure is exploited by us to segment it.

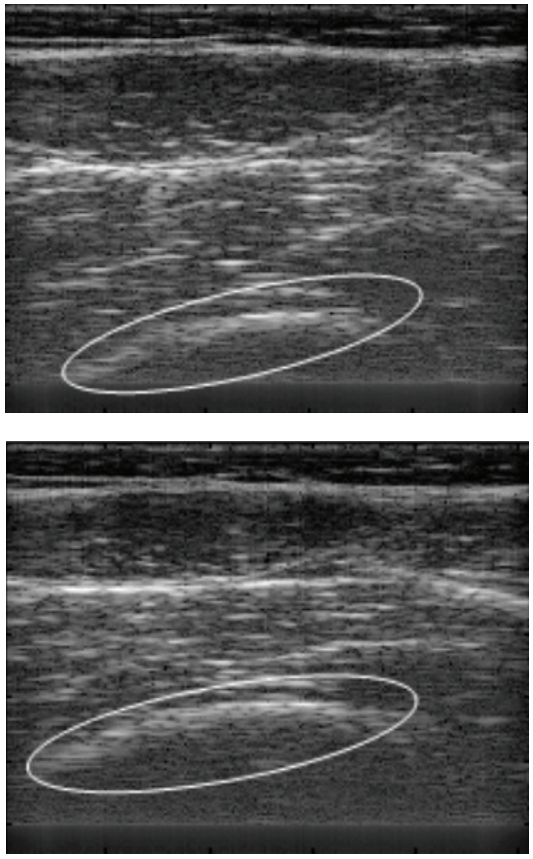

Fig. 4. Ultrasound image without pressure (a), ultrasound image with pressure (b). Both figures clearly show that the bone which is a rigid structure moves upwards (that is towards the transducer) when pressure is applied

In this part of the algorithm, we make use of the images from *triple shadow check* in which we scanned the echoes from the bottom towards the top in a straight line. So we have two such scanned images, one with pressure, and one without it.

Now, as we have observed a shift of the bone surface in figure 4, we expect a similar shift between the echoes coming from the bone surface. Figure 5 shows the echoes from the corresponding RF line of the two images. So both echoes come from the same corresponding positions in the images with and without pressure.

It can be easily observed in figure 5b that the echo which is from the image with pressure shifts to the left as compared to the echo in figure 5a which is from the image without pressure. This shift is very easy to understand if you assume the transducer to be at ‘0’ po-

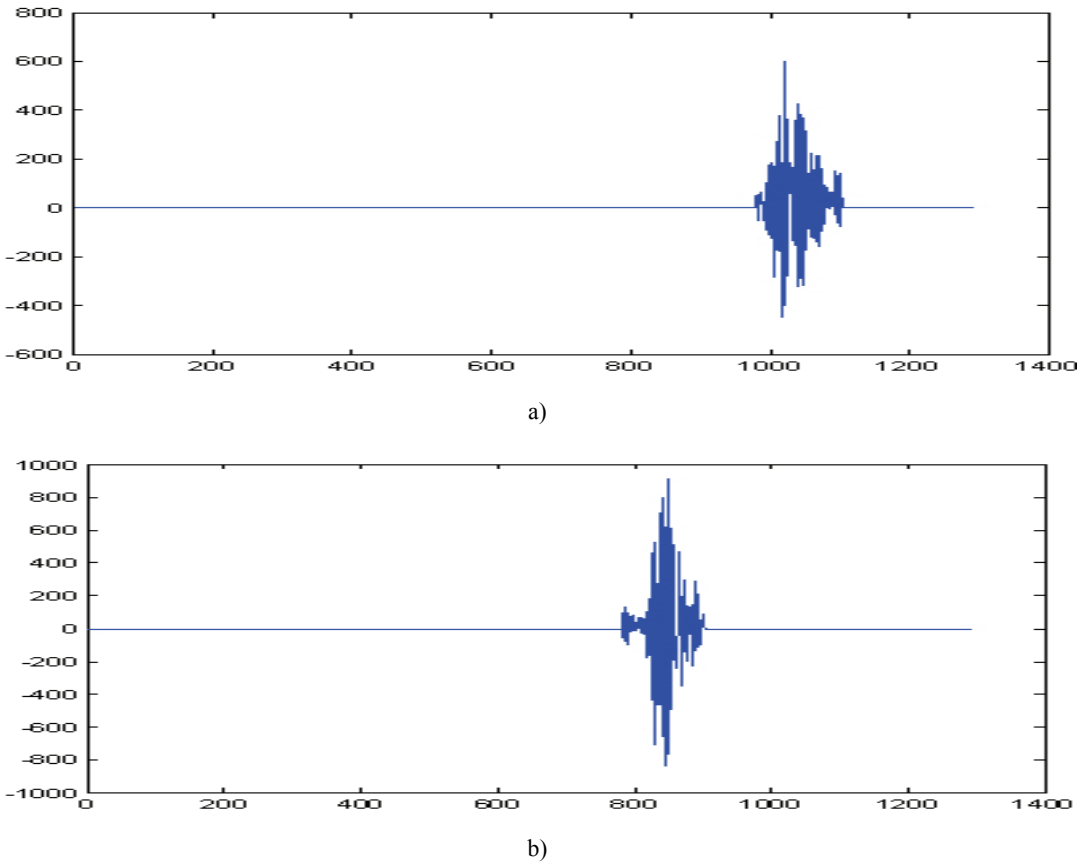

Fig. 5. RF signal at some location of the image without pressure after *bottom-up* procedure of *triple check* method (a), RF signal at some location of the image with pressure after *bottom-up* procedure (b). The *X*-axis represents the sample number, while the *Y*-axis represents calibrated voltages. Two echoes are expected to be from the bone as they are last echoes in respective RF lines. The transducer is moved to the extreme left and as we can see the echo in the RF line with pressure is shifted to the transducer that is to the left

sition of the *X*-axis. As the transducer moves to the right, the echoes appear to be moving to the left. Now these shifts are constant for all the echoes coming from the bone surface, because we have already discussed that the entire bone surface uniformly moves upwards in the image with pressure due to its hardness.

So we calculate all the shifts between the corresponding echoes of the image with and without pressure and we expect that this shift will be constant for the bone. We calculate this shift between the echoes applying the cross-correlation of the two corresponding signals from the image with pressure and the image without it.

After calculating the shifts we find the mean of the shift which is positive, i.e. is we consider only the shifts of the echoes to the left, because if the echo is shifting to the right in the RF line of the image with pressure, this means that the structure from which this echo comes is moving away from the transducer which is not true for the bone because bone is rigid and will remain in the same position.

This calculated mean is considered as a threshold and all the RF signal lines which have shifts of echoes less than this or have negative shifts are nullified. So after this procedure only those RF lines which have significant shifts of echo to transducer remain and the rest of the RF lines are rejected.

Now based on these RF lines we can calculate the position of the echo of the bone. As shown in figure 5b, the position of the echo is at the sample number 820 on the *X*-axis. Using these locations we draw a line on the B-mode image showing the bone. Since this line is a zigzag in shape, it should be smoothed out by taking an average of every 10 consecutive RF line positions.

Finally, we create the a third-order function and plot a smooth line to show the existence of bone in B-mode image. The above described workflow algorithm can be viewed in the form of a flow chart (figure 6).

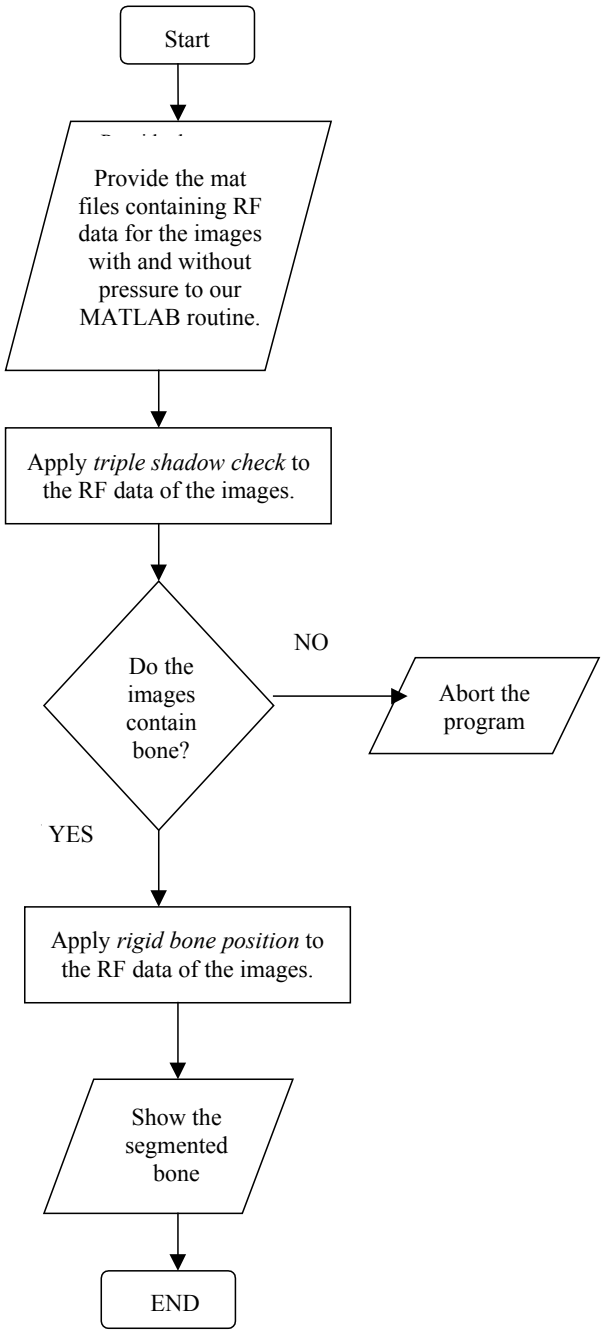

Fig. 6. Flow chart of the algorithm

3. Results

The algorithm works effectively for segmenting the bones in the 2D ultrasound images. The algorithm was tested for 120 images of human leg of different individuals and its usefulness proved to be satisfactory. Out of these test images 100 images were with bone, while 20 were without it.

Among these test images the algorithm detected 99 with bones and highlighted the bones for the same number of images. 21 were detected without bone. One image which had bone in it was detected without bone, while no image without bone was termed as "with bone" by the algorithm.

The results are tabulated as follows:

	With bone images	Without bone images
Bone detected	99	0
No bone detected	1	20

The sensitivity of the above test proves to be (99/(1 + 99)) = 0.99, while its specificity is (20/(0+20)) = 1.

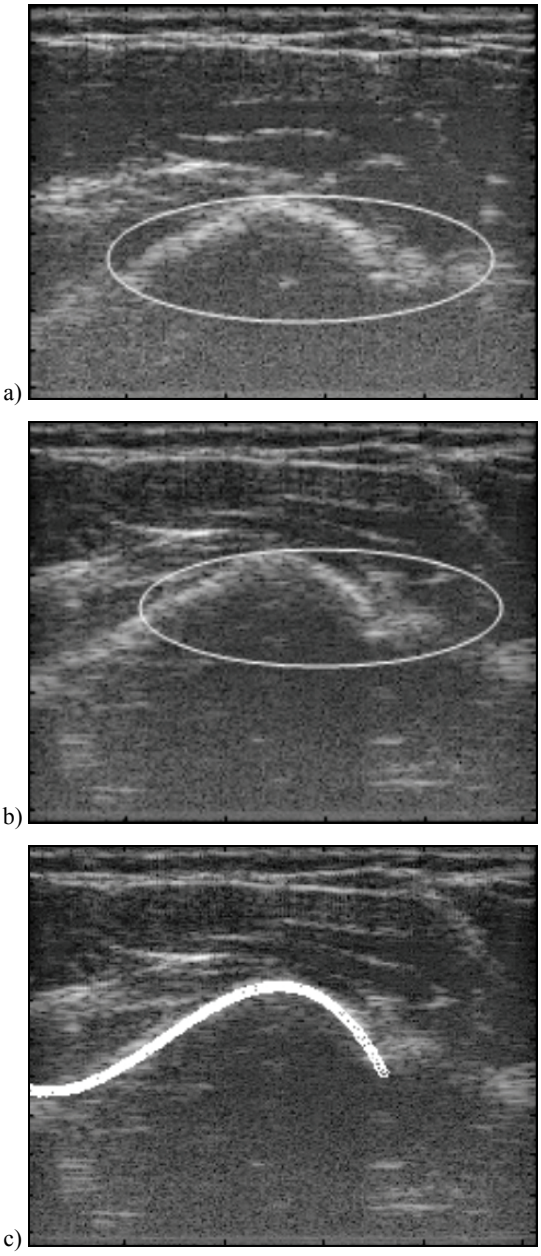

Fig. 7. Ultrasound image without pressure (a), ultrasound image with pressure (b), bone segmentation (c). The line indicates the bone surface

We demonstrate some of our results in three parts. The oval represents the bone. First we show the bone which is at a certain depth in the 2D ultrasound image. The thick white line always shows the segmented bone. We always highlight the bone in the ultrasound image with pressure because this image has clearer bone surface as compared to the bone surface without pressure.

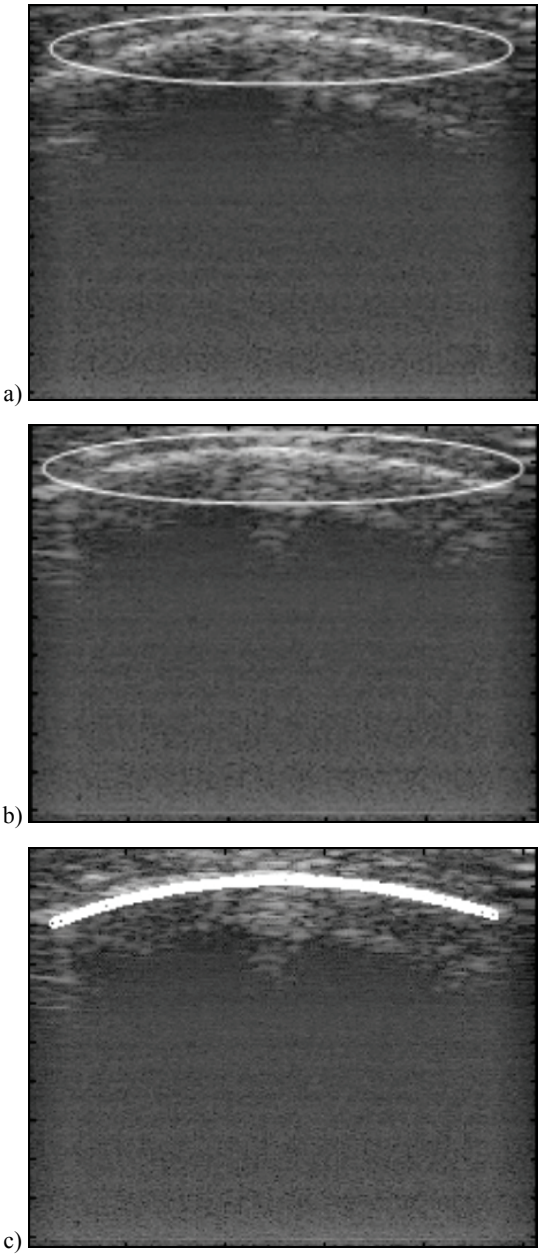

Fig. 8. Ultrasound image without pressure (a), ultrasound image with pressure (b), bone segmentation (c). The line shows the bone surface

Now in the second part of the results obtained, we concentrate on the bone which is in close proximity to the probe. In this case, we do not deal with a sufficient movement of the bone structure as there are no muscles or fat between the probe and the bone. The results for such a case are given in figure 8.

In the third part of our results, we try to demonstrate the result of our algorithm when there is no bone echo in the ultrasound image.

Fig. 9. The final image after *bottom-up semi-compound shadow* method

Figure 9 shows the final image of *triple check* method obtained by logical summarizing (OR) the images with and without pressure. As we can see, there is no similar significant structure in the shadow of the structures detected by the algorithm. The significant structure is shown by oval. So the algorithm reports that there is no bone echo in these images.

4. Discussion

This algorithm describes the method of segmenting bone using RF data. The main purpose of this algorithm is to obtain a perfect bone surface from a 2D ultrasound image. But as we may observe it is very difficult to identify the bone structure in a single ultrasound image. Unlike CT or X-ray, the bone is not the only hyperechogenic structure in the image. But the structure brightness depends on the amount of ultrasound reflected by this structure in the body. So it is possible that a tendon or a muscle may appear brighter than a bone if the former is nearer to the ultrasound probe than the bone. Thus, the difficult task is to identify and isolate the bone structure amongst a number of bright structures in the ultrasound image. However, based on the results obtained, we can see that our algorithm very accurately differentiates bone structures from the other body tissues in the image. If the ultrasound image does not contain bone structures either, the algorithm is efficient enough to isolate such ultrasound images.

Image processing has always been the most favourite method for segmenting structures in an image. But for our algorithm we do not use any image processing of the B-mode image. All the procedures are performed using the RF data obtained from the ultrasound device. This mean that we perform only signal processing based on the RF data.

The *rigid bone position* requires specifically the use of RF data, as we need to observe the shift in the echo from the bone. For calculating this shift we cross-correlate the corresponding signals of the images with and without pressure. This is not possible based on the gray level values in the ultrasound B-mode image. Cross-correlation is the heart of this algorithm. We cross-correlate the corresponding signals of the image with and without pressure to identify the shifts between the echoes. We gather all the echoes which have constant shifts and those are the echoes from the bone structure, as bone being a rigid body will not change its shape and so it will move uniformly in one direction. Hence, we have constant shifts between all the echoes from the bone structure. While the corresponding echoes from other soft structures like skin and muscle will not have constant shifts as they bend due to the low pressure applied at the ultrasound probe.

This algorithm could be extremely helpful for the 3D reconstruction of bone structures. The present technique is not based on noninvasive or cheap methods for intraoperative measurements of the geometry of arms and legs. They can be performed by using X-rays (which are injurious) and CT-scans (are expensive). The cheapest method is the ultrasound method. But for constructing the 3D image of a bone the first thing required is a very good segmentation of bone contour in a 2D ultrasound image, and this should be the 2D navigated ultrasound image of the 3D bone object. This means that the 2D ultrasound images need the position and the orientation in the patient's co-ordinate system. Using these segmented bone structures, the 3D reconstruction of bone is undertaken which can be very useful for visualizing pathological deformities like leg deformity preoperatively, intraoperatively and postoperatively to check finally the results of surgery.

This algorithm very well overcomes the limitation of sonography in imaging bone structures. Such limitations as the steering of energy by bone structures in the wrong direction and the other structures appearing brighter than the bone do not influence the *rigid bone position* and *triple check* methods and allow the bone to be segmented.

Using these 2D segments, the 3D bone visualization would be far better for the corrective osteotomy than the 2D bone visualization from fluoroscopy (C-Arm) as the bone visualization is 3-dimensional, and not 2-dimensional.

5. Conclusion

In conclusion one can say that our algorithm very successfully segments bone echo in a 2D ultrasound image. In terms of a future scope of this work, these 2D segmented bones can be navigated and combined to form a 3D reconstruction of bone. This visualization of bone using sonography has a lot of advantages compared to computed tomography in the pre-, intra- and postoperative measurements of bone deformity for corrective osteotomy. Also this visualization does not make use of any B-mode segmentation.

References

[1] AMIN D.V., KANADE T., DiGIOIA A.M. 3rd, JARAMAZ B., *Ultrasound based registration of the pelvic bone surface for surgical navigation*, First Annual Meeting of International Society for Computer Assisted Orthopaedic Surgery (CAOS-International), Davos, Switzerland, 2001, p. 36.

[2] THOMAS J.G., PETERS R.A. III, JEANTRY P., *Automatic Segmentation of ultrasound images using morphological operators*, IEEE Trans. Med. Imag., 1991, 10(2), 180–186.

[3] DAANEN V., TONETTI J., TROCCAZ J., *A fully automated method for the delineation of osseous interface in ultrasound images*, [in:] *Medical Image Computing and Computer-Assisted Intervention (MICCAI)*, Springer-Verlag, Berlin, 2004, 549–557.

[4] JAIN A.K., TAYLOR R.H., *Understanding bone responses in B-mode ultrasound images and automatic bone surface extraction using a Bayesian probabilistic framework*, [in:] *Medical Imaging 2004: Ultrasonic Imaging and Signal Processing*, Walker W.F., Emelianov S.Y. (eds.), Proc. SPIE 2004, 5373, 131–142.

[5] KEPPLER P., STRECKER W., CLAES L., *Die sonographische Bestimmung der Beingeometrie*, Orthopäde, 1999, Vol. 28, 1015–1022.

[6] KOWAL J., AMSTUTZ C.A., NOLTE L.P., *On B-mode ultrasound based registration for computer assisted orthopaedic surgery*, First Annual Meeting of International Society for Computer Assisted Orthopaedic Surgery (CAOS-International), Davos, Switzerland, 2001, p. 35.

[7] KRUEGER M., PESAVENTO A., ERMERT H., HILTAWSKY K.M., HEUSER L., ROSENTHAL H., JENSEN A., *Ultrasonic strain imaging of the female breast using phase root seeking and three-dimensional "optical flow"*, IEEE Proceedings Ultrasonics Symposium, 1998, 2, 1757–1760.

[8] LORENZ A., SOMMERFELD H.J., GARCIA-SCHURMANN M., PHILIPPOU S., SENGE T., ERMERT H., *A new system for the acquisition of ultrasonic multicompression strain images of the human prostate in vivo*, IEEE Trans. Ultrason. Ferroelect. Frequency Contr., 1999, Vol. 46, No. 5, 1147–1154.

[9] MURATORE D.M., DAWANT B.M., GALLOWAY R.L. Jr, *Vertebral surface extraction from ultrasound images for technology-guided therapy*, Proceedings of Medical Imaging. Bellingham, WA: SPIE, 1999, 1499–1510.

[10] OPHIR J., CÉSPEDES I., PONNEKANTI H., YAZDI Y., LI X., *Elastography: A quantitative method for imaging the elasticity of biological tissue*s, Ultrasonic Imaging, 1991, 13, 111–134.

[11] OVERHOFF H.M., LAZOVIC D., von JAN U., *Vizualization of newborn's hip joint using 3-D ultrasound and automatic image processing*, Proc. International Symposium on Medical Imaging, 1999.

[12] PESAVENTO A., PERRY C., KREUGER M., ERMERT H., *A time-efficient and accurate strain estimation concept for ultrasonic elastography using iterative phase zero estimation*, IEEE Trans. Ultrason. Ferroelect. Frequency Contr., 1999, Vol. 46, No. 5, 1057–1067.

[13] PESAVENTO A., LORENZ A., SIEBERS S., ERMERT H., *New real-time strain imaging concepts using diagnostic ultrasound*, Phys. Med. Biol., 2000, 45, 1423–1435.